JOURNAL OF SPACECRAFT AND ROCKETS
Vol. 31, No. 3, May–June 1994

Dynamics of a Space Module Impacting Water

J. R. Brooks* and L. A. Anderson†
University of Central Florida, Orlando, Florida 32816

The dynamic response of a Water Landing Space Module (WLSM) during impact upon water was investigated. A 1/5th-scale model was tested in a water tank and the results were compared with those attained using analytical techniques and computer simulations. A knowledge of the response of the WLSM during impact is necessary to identify design choices that are within the physical limitations of crew members and materials. The purpose of this research was to use simulations to establish trends that occur when the variables of entry speed, angle, and weight are varied. Results suggest which initial conditions of the full-scale WLSM keep impact accelerations under specified limits.

Nomenclature

a = distance from pivot point to CG, in.
b = outside accelerations, in./s^2
g = acceleration due to gravity, in./s^2
I = moment of inertia, lb$_f$s^{2}in.
L = distance from top of the model to the center of gravity (CG), in.
m = mass of model, slugs
t = time, s
V = volume, in.^{3}
V_0 = reference volume, in.^{3}
v = velocity, in./s
w = weight, lb
x = displacement, in.
θ = angular displacement, rad
λ = length scale factor

Introduction

STUDIES of the impact phenomena[1-4] based on the theoretical work by von Kármán[1] resulted in equations for the impact of rigid bodies upon a fluid. The von Kármán approach assumed the reaction of the water was due solely to its inertia. Using an expression for the added apparent mass due to the water, the accelerations and pressures affecting the rigid body were determined. The studies cited in Refs. 2–4 used a modified version of the von Kármán theory.

Kaplan[5] examined the specific problem of the Apollo Command Module (ACM) impacting water. Kaplan discovered that the flexible heat shield has a strong effect on the accelerations experienced by the vehicle. The flexible heat shield increases the amplitude of the peak acceleration. To account for the flexible heat shield, Kaplan used a mathematical model consisting of two masses attached by a spring. To avoid the problem of infinite pressures at impact, Kaplan incorporated an imaginary cone on the bottom of the heat shield. From theory and experiment, he found that the peak acceleration is proportional to the square of the impact velocity. Kaplan's theoretical results correlated well with full-scale ACM impact tests.[5]

Recent efforts to solve the impact problem have produced a solution for the impact problem based on finite elements.[6,7] Geers et al.[6] developed a technique that treats the fluid response in terms of the fluid motion rather than in terms of the fluid volume or added apparent mass. The fluid is considered inviscid and incompressible and the free surface is simulated by a finite-element mesh. Solutions for a wedge and cylinder impacting water correlate closely with the data from actual experiments. In the finite-element study by Mansour and Seireg,[7] the water is simulated as an elastic material with special elements to deal with situations where the fluid undergoes large displacements.

A finite element program, Nonlinear Dynamic Analysis of Structures in Three Dimensions, (LS-DYNA3D), was used in this work to simulate the impact of the WLSM upon water. This program was developed by Hallquist[8] at Livermore Software Technology Corporation (LSTC) and is especially useful because of the contact-impact interface algorithm it contains.

Water Landing Space Module Scale Model

The 1/5th-scale working model built for testing simulates the dynamic behavior of an ACM-based WLSM. The construction involved three primary considerations: geometric and dynamic similitude, method for modeling the center of gravity (CG) and mass moment of inertia, and shell construction. Several options were investigated for each consideration and the chosen solutions are presented hereafter.

Geometric and Dynamic Similitude

The model was scaled down to 1/5th using the Froude model scaling technique for model testing.[9] The scaling technique transforms model quantities to prototype quantities and vice versa. Scaling factors for model variables are listed in Table 1. The full-scale dimensions for the WLSM are shown in Fig. 1. The CG and mass moment of inertia (I) of the WLSM model are shown in Table 2. Full-scale and 1/5th-scale values are based on the ACM. The radius around the base of the WLSM is larger and the curvature of the heat shield for the WLSM is smaller than the ACM. Consequently, the weight and mass moment of the WLSM is larger.

Center of Gravity and Mass Moment

Three flat, circular plates were used for modeling both the CG and mass moment of inertia of the WLSM (Fig. 2), a fixed

Table 1 Model scaling factors

Variable	Symbol	Scale Factor	Value
Length, in.	L	λ	0.2
Acceleration of gravity, in./s^2	g	1.0	1.0
Mass, slugs	m	λ^3	0.008
Mass moment of inertia, lb$_f$s^{2}in.	I	λ^5	0.00032
Time, s	t	$\lambda^{1/2}$	0.4472
Displacement, in.	x	λ	0.2
Linear velocity, in./s	v	$\lambda^{1/2}$	0.4472
Linear acceleration, in./s^2	b	1.0	1.0
Angular rotation, rad	θ	1.0	1.0

Received Jan. 18, 1993; revision received May 14, 1993; accepted for publication June 1, 1993.

*Research Engineer, Rockwell Research Fellow.
†Associate Professor, Mechanical and Aerospace Engineering. Associate Fellow AIAA.

Table 2 Water Landing Space Module model properties

Properties	1/5th-scale model	Full-scale prototype
I_x	40.75 $lb_f s^2 in.$	127355 $lb_f s^2 in.$
I_y	40.75 $lb_f s^2 in.$	127355 $lb_f s^2 in.$
I_z	18.53 $lb_f s^2 in.$	57912 $lb_f s^2 in.$
X_{CG}	1.24 in.	6.2 in.
Y_{CG}	0.0 in.	0.0 in.
Z_{CG}	4.56 in.	22.8 in.
w	131 lb.	16375 lb.

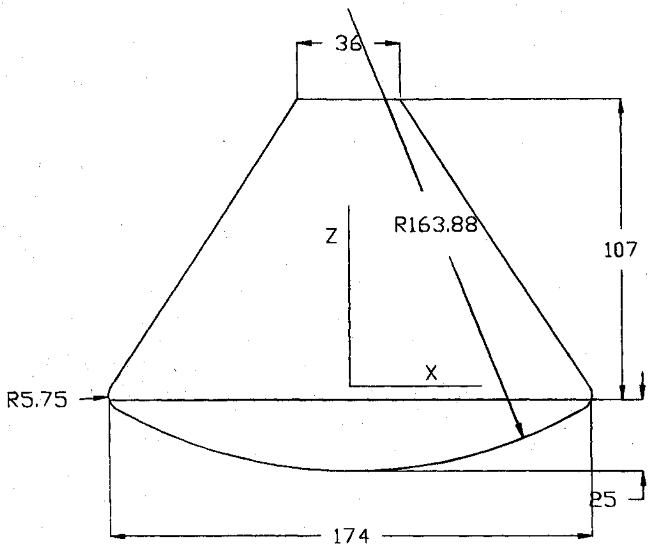

Fig. 1 Full-scale WLSM dimensions (in.).

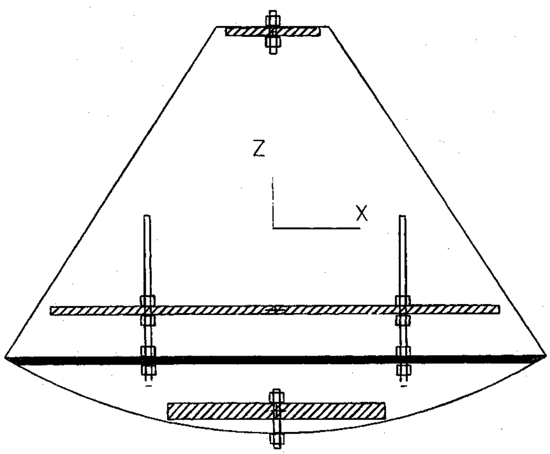

Fig. 2 Mass moment of inertia system.

flat plate mounted inside the top of the shell, a second fixed plate at the base of the shell, and a movable plate at the floor of the model. The three flat, circular plates are treated as a concentrated mass with local CG at the centroid of the plates. By varying the position of the center plate, the CG of the model is altered for testing. To determine the size of the plates, the CG and moment of inertia of the empty model was determined. Nonhomogeneities and asymmetry of the constructed shell required empirical determination of the exact values of the weight, CG, and mass moment of inertia. The mass was measured by weighing the model on a scale. The location of the CG and the magnitude of the mass moment of inertia were then measured by suspending the model from a wire and recording the period of oscillation as it was swung pendulum-wise from the top and then from the bottom of the model.

The data from the experiment was used to calculate the actual CG and mass moment of inertia of the model. Equations for determining the CG and mass moment of inertia were developed by summing the moments in a simple pendulum relationship.

$$(I_G + ma^2)\,\ddot{\theta} + mga\sin\theta = 0 \qquad (1)$$

From these experiments, the amount of weight and moment of inertia the plates needed to contribute was determined.[10] The plate system configuration is described in Table 3. The middle plate was bolted to the floor of the WLSM model using a system of four studs, spacers, and washers. The plate has a horizontal range from 0 to 3.0 in away from the model hatch. A series of spacers on the studs allows vertical variation of the plate. The floor can be rotated 180 deg to permit a vertical range of approximately 9 in.

Shell Construction

To satisfy the requirements of strength in all directions, low weight, and water tightness the WLSM model shell was constructed of fiberglass.[11] Tests were performed to verify fidelity. The model's final properties are shown in Table 4. The dimensions are within the range of possible WLSM designs.

Model Testing

The objective of the drop tests performed by the University of Central Florida (UCF) at O.H. Hinsdale Wave Research Laboratory at Oregon State University (OSU), was to determine the accelerations of the model upon impact with water. Data was recorded by two accelerometers placed at the CG of the model, one in the vertical direction and one in the horizontal direction. The accelerometers were connected to a data acquisition system and calibrated. The model was then placed on a cable and trolley system (Fig. 3) designed to give the model the desired entry speed and angle at impact.

Desired velocities for each test were scaled down as shown in Table 1. As shown in Fig. 3, the values of (H) and (L) needed to achieve the desired velocity were then determined. With the model in position the cord holding the model was cut. After traveling a predetermined distance, the release cord pulled back on the hook and the model dropped into the water. Data was gathered over a range of impact angles by hanging the model from the trolley at different angles.

Impact Tests

Thirteen drop tests were performed at OSU with entry angles from 0.0 to −90 deg. The resultant impact velocities varied from 10.7 to 18.8 fps. These tests were performed using the same CG and mass moment configuration. Since it was impossi-

Table 3 Plate system configuration

Plate location	Inner radius, in.	Outer radius, in.	Thickness, in.
Top plate	0.0	3.0	0.5
Middle plate	4.5	9.0	1.0
Bottom plate	0.0	4.5	1.25

Table 4 Properties of 1/5th-scale Water Landing Space Module model

Variable	Value
Hemispherical base height, in.	5.5
Hemispherical base diameter, in.	35.75
Conical section height, in.	22.25
Conical section diameter, widest pt.(in.)	35.75
Conical section diameter, narrowest pt.(in.)	7.0
Model weight, lb	131
Model moment of inertia, slug ft^2	3.39

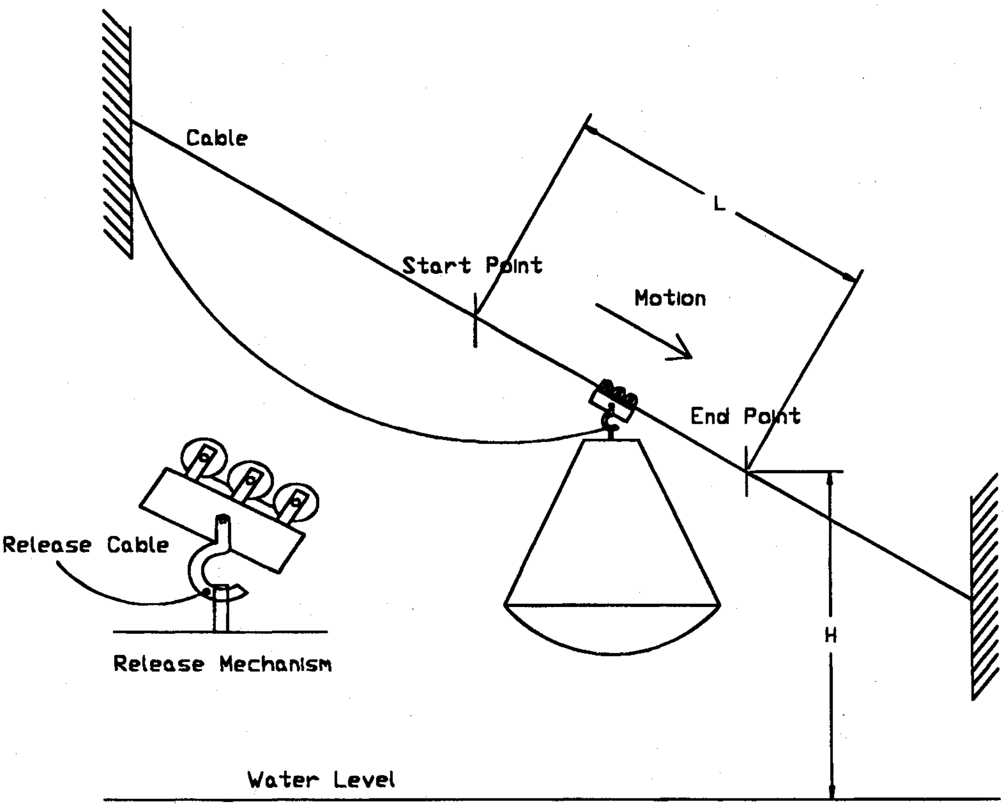

Fig. 3 Drop mechanism.

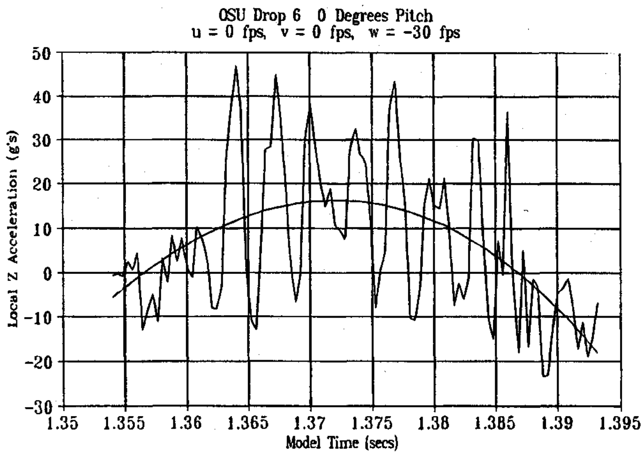

Fig. 4 Typical drop data with curve fit.

ble to predict exactly where on the wave the model might impact, all tests were performed in simulated calm seas.

Impact Test Results

Roughly three seconds of data, with a sampling rate of 2500 Hz, were recorded for each test. The testing equipment was calibrated in the first few tests. The peak accelerations from the experiments were larger than expected. This amplification was due primarily to structural vibration of the model. The accelerometers were mounted to the floor of the model and the floor was attached to the model by its outer edges. To account for structural vibrations, a curve fit was applied to the output through a polynomial regression technique. The order of the polynomial was chosen from the appearance of the data and coefficients of the polynomial were determined by applying the least-squares criterion.[12] Figure 4 shows a typical plot of experimental output with a curve fit. These results were used to confirm the validity of the DYNA3D software.

Verification of Finite Element Software

The software used for this project consisted of three separate programs: INGRID, a preprocessor; DYNA3D, a finite element program; and TAURUS, a postprocessor. INGRID was used to generate the geometry, initial conditions, and loads for the model.[13–15] Once the model was created, the information was input to DYNA. This program performs the finite-element analysis and creates databases containing the output from the analysis. DYNA uses the standard finite-element approach, where the geometry, loading, and material properties are all known.

The DYNA program was verified against proven analytical results for an impact into water. Kaplan's equations were directed specifically towards the ACM and his results correlated well with full-scale drops.[5] Kaplan's development was used to verify the DYNA software by creating an ACM model for DYNA and running the same conditions Kaplan used in his analytical equations.

The model of the vehicle was generated using the INGRID preprocessing package. A model of the Apollo Command Module and water was created by Stillman of Livermore Software Technology Corporation (LSTC) for Rockwell International. This model was used as a starting point for the WLSM models generated at UCF. The capsule was created from shell elements, with a rigid body material designation. All objects with this material type moved as one body. The moment of inertia and center of gravity of the rigid material are defined by the user instead of being calculated by the program from the model geometry. The capsule for the Kaplan tests had the dimensions shown in Fig. 5. The capsule was created by combining a cone, torus, and sphere constructed with the proper dimensions and joined at specific coordinates. The Kaplan model had the mass characteristics shown in Table 5.

DYNA does not have computational fluid capabilities, therefore the water was simulated using a 200 × 100 × 100 in. block of solid brick elements. The edges of the block were defined as nonreflecting boundaries allowing the water block to be relatively small in size. These elements were given the null hydrodynamic material type which allowed a new equation

Table 5 Kaplan model properties

Properties	Kaplan model
I_x	67536 lb$_f$s^{2}in.
I_y	63708 lb$_f$s^{2}in.
I_z	57912 lb$_f$s^{2}in.
X_{CG}	4.5 in.
Y_{CG}	0.0 in.
Z_{CG}	41.4 in.
w	12250 lb

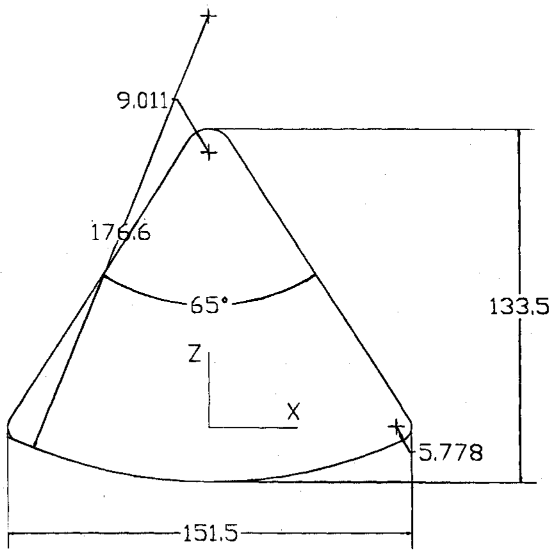

Fig. 5 Kaplan model dimensions (in.).

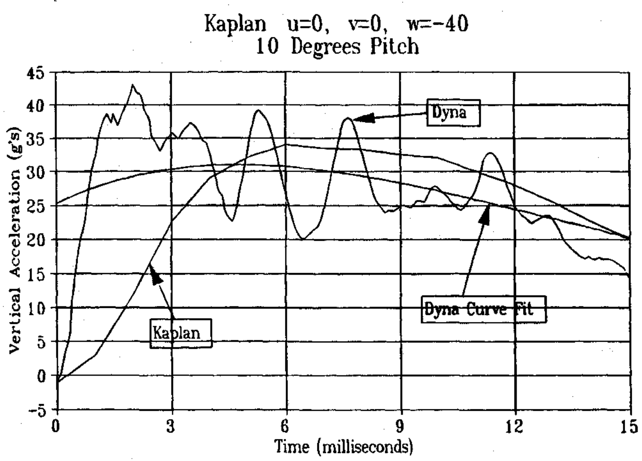

Fig. 6 Typical DYNA plot with curve fit.

of state to be specified. The Gruneisen[8] equation of state was used to simulate the behavior of water. To complete the model, a constant body force was applied to the entire model to simulate the effect of gravity.

After the Kaplan configuration was run through the software, the results were compared to the results from Kaplan's analytical equations. A typical DYNA plot of vertical acceleration vs time is shown in Fig. 6. A variety of entry angles and entry speeds were tested to compare against the Kaplan results. To compare the results between the Kaplan and DYNA models, a percent deviation for each maximum acceleration was calculated. This was performed by dividing the difference between the two by the Kaplan result. A comparison of DYNA and Kaplan results is shown in Table 6. All Kaplan tests shown had no component of horizontal velocity. The percent deviation ranges from 1.92 to 26.3, generally favoring the lower entry angles.

UCF Experiments Performed at OSU

In comparing the results from the impact tests performed at OSU with the same conditions using DYNA, dimensions of the DYNA model were changed to the scaled-up geometry of the WLSM model. These dimensions are shown in Fig. 1. A comparison of DYNA results and OSU results is shown in Table 7.

The results show two tests with invalid horizontal components of velocity. The dropping mechanism used for the experiments induced a rotational movement that decreased the accelerations felt at impact. The amount of rotational movement imparted to the model could not be determined from the data collected during the experiments, therefore these tests could not be accurately reproduced using DYNA.

Finite-Element Tests

To identify the behavior of the craft at impact, simulations were performed on the software over a wide range of conditions. The characteristics of entry speed, entry angle, and vehicle weight were varied. The new geometry for the WLSM used for these tests is shown in Fig. 7. The mass properties are shown in Table 8.

The given values were entered in the DYNA model. For each test a total of 500 data states were created from the simulation. Displacement, velocity, and acceleration of the model were recorded at each data dump. An important result from these tests is the peak acceleration experienced by the craft upon impact. Each test output has been curve fit to remove peaks caused by modeling the water. The following tests report the accelerations as defined by the local coordinate system of the craft. All of the figures in the following sections show the accelerations in the local Z direction, unless indicated otherwise. All velocities are represented using u, v, and w to denote velocity components in the x, y, and z directions, respectively. Velocities are measured in the units of feet per second (fps). The local coordinate system moves with the model in the position shown in Fig. 7.

Vary Vertical Velocity

The vertical velocities ranged from 5 to 35 fps with a 5 fps interval. A test at 7.5 fps is included, because this was determined to be the nominal speed at which the WLSM would be traveling upon impact. The lower velocity values were based on retro rockets slowing the vehicle down. The higher velocity values were based on a minimal number of parachutes slowing the vehicle down. Figure 8 shows the acceleration in g vs time for all of the vertical velocity tests. These graphs indicate the trend of impact g's being higher and happening sooner with a higher entry speed.

Vary Entry Angle (Pitch)

To determine the effect of varying the entry angle of the WLSM upon impact, the entry angle was varied from −10 to 35 deg. Pitch angle is measured as shown in Fig. 9. Results from these tests are shown in Fig. 10. These tests show the impact acceleration can be reduced by having the WLSM enter the water with a nonzero pitch angle. The impact acceleration tends to decrease as the entry angle is increased. All accelerations appear very low because of the small entry speed of 7.5 fps.

Vary Vehicle Weight

The effect of altering the vehicle weight was determined by testing weights ranging from 14,000 to 18,000 lb. When weight increases, normally the mass moment of inertia of the vehicle also increases. To accommodate this, the moment was increased linearly according to the rise in weight. The weight and mass moment of the ACM and of the WLSM design were used as the two points to establish a linear relationship. The test results shown in Fig. 11 demonstrate that the impact acceleration is less for heavier craft. All accelerations are low due to low entry

Table 6 DYNA vs Kaplan results for rigid-body impact

Vertical velocity, fps	Entry angle, deg	DYNA maximum acceleration global Z, g	Kaplan maximum acceleration global Z, g	Percent deviation
25	10	13.25	13	1.92
30	10	17.7	19	6.84
40	10	31	33	6.06
25	15	10.96	12	8.67
30	15	17.59	18	2.28
40	15	28.49	33	13.67
25	20	8.83	7	26.1
30	20	12	11	9.09
40	20	24	19	26.3

Table 7 Summary of UCF impact tests performed at OSU

Horizontal velocity, fps	Vertical velocity, fps	Entry angle, deg	DYNA maximum acceleration local Z, g	OSU maximum acceleration local Z, g	Percent deviation
0	24	0	9.41	10.54	10.72
0	24	15	8.46	6.97	21.38
20	27	30	4.1	1.37	199
0	30	0	15.1	16.28	7.25
0	30	15	13.83	6.87	101
0	30	30	6.01	4.9	22.7
30	30	30	5.04	2.767	82.1

Table 8 Model properties

Properties	
I_x	81804 $lb_f s^2 in.$
I_y	79620 $lb_f s^2 in.$
I_z	72444 $lb_f s^2 in.$
X_{CG}	8.8 in.
Y_{CG}	0.0 in.
Z_{CG}	49.6 in.
w	15575 lb

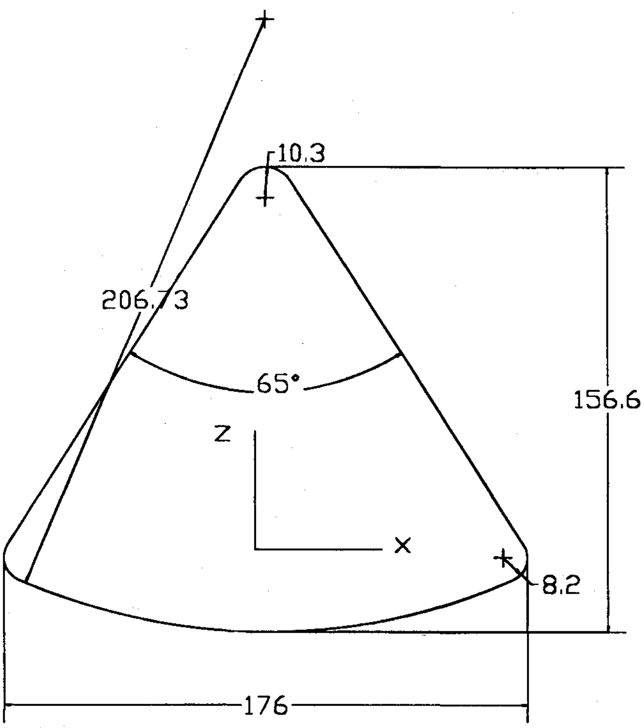

Fig. 7 New WLSM dimensions (in.) with local coordinate system.

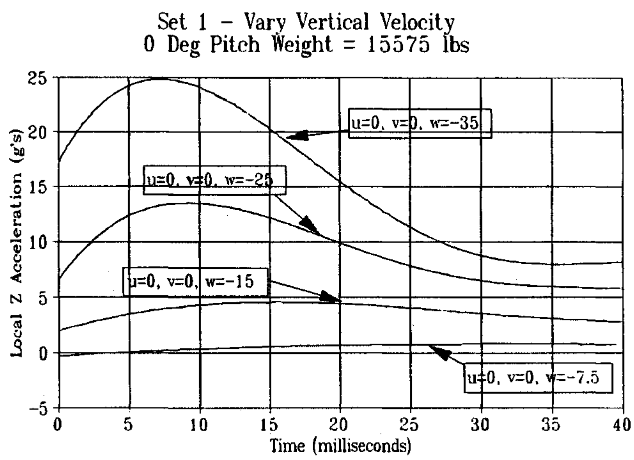

Fig. 8 Acceleration vs time for vertical velocity tests.

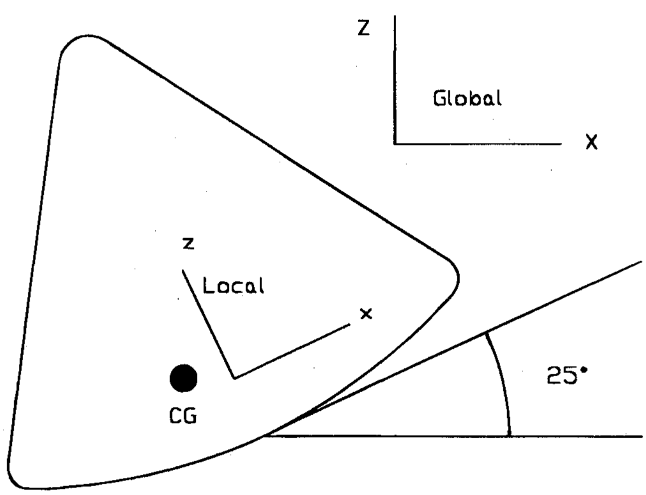

Fig. 9 Pitch angle measurement.

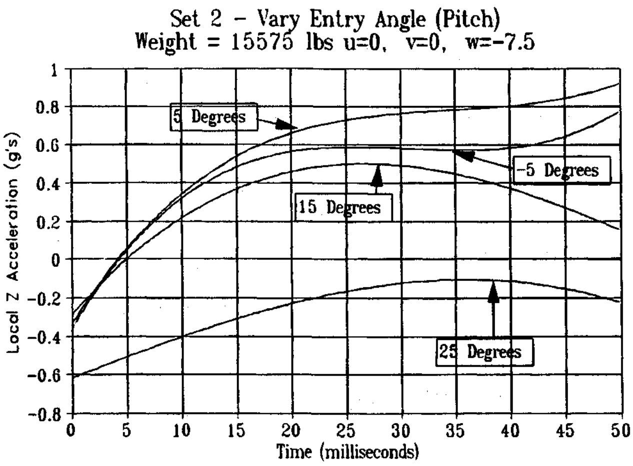

Fig. 10 Acceleration vs time for pitch tests.

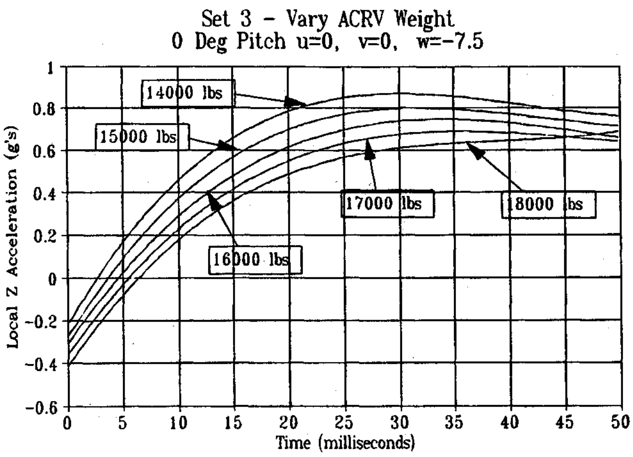

Fig. 11 Acceleration vs time for weight tests.

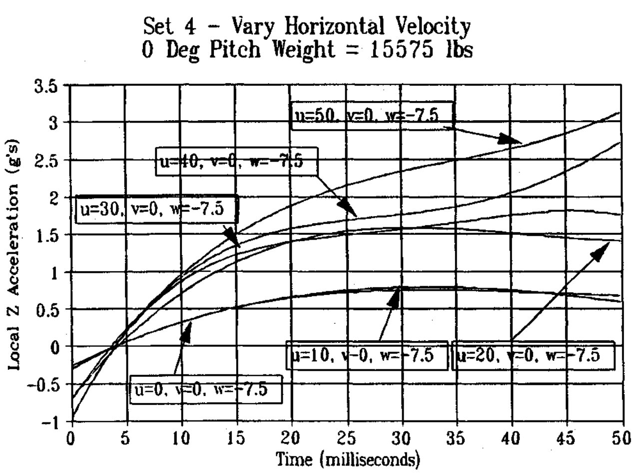

Fig. 12 Acceleration vs time for horizontal velocity tests.

velocity. The general trend shows a small advantage gained in reduced g force for a large increase in weight.

Vary Horizontal Velocity

The component of horizontal velocity ranged from 0 to 50 fps. The results from these tests can be seen in Fig. 12. The majority of these plots are grouped close together. This implies that a horizontal component of velocity has little effect on the acceleration in the local Z direction. However, this component of velocity effects accelerations in the local X direction as

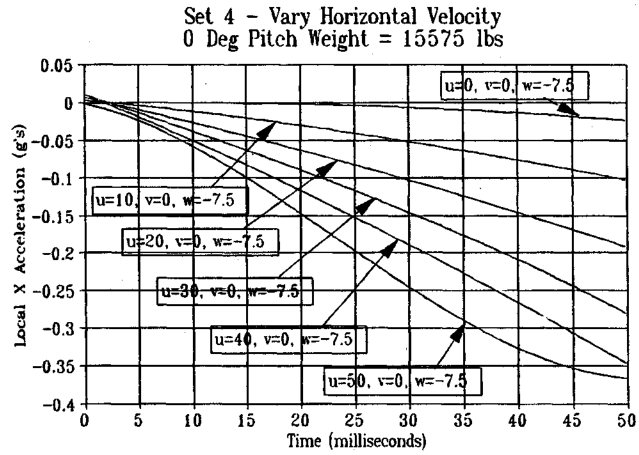

Fig. 13 Acceleration vs time for horizontal velocity tests.

shown in Fig. 13. The local X accelerations increase as the velocity in the local X direction increases. The validity of simulating impacts with horizontal component of velocity using DYNA has not been established through model testing or analytical techniques at this time.

Observations and Recommendations

The analytical approaches put forth by von Kármán, Li and Sigimura, Kaplan, and others provide us with the beginnings for a complete solution of the impact phenomena through use of numerical techniques such as finite elements. This work, simulating impact using finite elements, demonstrates some of the problems encountered when modeling water. DYNA3D simulated the behavior of water accurately for a short period of time, but did not correlate well after the first 30–40 ms. The initial period of time was long enough to establish trends occurring under a range of conditions. The effects of varying the vertical velocity, entry angle, vehicle weight, and horizontal velocity were identified. These trends help establish the conditions that must be avoided during a water landing. For example, if a sick or injured crew member can not sustain an impact of over five g, these results reveal which initial conditions keep the acceleration under the specified limits.

Several areas have been shown to need further investigation. Model testing is needed over a wider range of conditions to include improved tests which vary the speed, weight, and entry angle. The model used for impact tests should be specifically designed to avoid structural vibrations. The ideal model would be a completely rigid body. The 1/5th-scale model used in this research was originally a flotation model for pitch and stability testing and allowed unwanted structural vibrations during impact tests. A better technique is needed for imparting the initial pitch and velocity to the model. The cable and trolley system imparted an unwanted model rotation during tests with horizontal velocity. In addition, cable tension had to be high to minimize velocity reduction during tests. A swinging pendulum system consisting of a two-bar linkage attached to a constantly horizontal platform may eliminate these problems, and deserves further investigation. The development of a more accurate numerical solution should be pursued. The possibility of combining a finite-element package with a computational fluids package is attractive for this purpose. A computational fluids package could more accurately simulate the behavior of the water. Livermore Software Technology Corporation is currently working on a computational fluids section to add to the DYNA software. If successful, DYNA may be able to more accurately simulate the phenomena of impact into water.

Acknowledgments

Appreciation is expressed to Rockwell Space Systems Division for supporting the Rockwell Graduate Fellowships that made this work possible. A portion of this work was supported by NASA and the Universities Space Research Association, to whom appreciation is expressed. The authors gratefully acknowledge the assistance of Raymond C. Manion, W. Robert Mason, Peter Kondis, Don Morris, and John McKinney of Rockwell International's Space Systems Division in preparing this document and discussing many of the computational and testing ideas contained herein.

References

[1] Albano, E., and Pohlen, M. J., "A Method for Determining the Dynamics of the Apollo Command Module at Sea," SID 63-466, North American Aviation Inc., Downey, CA, May 1963.

[2] Li, T., and Sigimura, T., "Study of Apollo Water Impact: Final Report, Hydrodynamic Analysis of Apollo Water Impact," Volume 1, SID 67-498, North American Aviation Inc., Downey, CA, May 1967.

[3] Wilkinson, J. P. D., Cappelli, A. P., and Salzman, R. N., "Study of Apollo Water Impact: Final Report, Dynamic Response of Shells of Revolution During Vertical Impact Into Water—Hydroelastic Interaction," Vol. 3, SID 67-498, North American Aviation Inc., Downey, CA, May 1967.

[4] Kettleborough, C. F., "Hydrodynamic Water Impact: Final Report," Texas Agricultural and Mechanical Univ., NASA CR-137370, March 1972.

[5] Kaplan, A., "Simplified Dynamic Analysis of Apollo Water Impact, Including Effects of the Flexible Heat Shield," 11176-6004-R0-00, TRW, Redondo Beach, CA, Sept. 1968.

[6] Geers, T. L., Loden, W. A., and Yee, H. C., "Boundary-Element Analysis of Fluid-Solid Impact" *Computational Methods for Fluid-Structure Interaction Problems,* American Society of Mechanical Engineers, New York, 1977, pp. 125–138.

[7] Mansour, A., and Seireg, A., "A Computer-Based Simulation of Ice-Breaking by Impact," *Journal of Energy Resources Technology,* Vol. 105, Dec. 1983, pp. 448–453.

[8] Hallquist, J. O., *LS-DYNA3D User's Manual*, Livermore Software Technology Corp., Waverly, CA, Jan. 1991.

[9] Baker, W. E., Westine, P. S., and Dodge, F., *Similarity Methods in Engineering Dynamics,* Hayden Book Co., Rochelle Park, New York, 1973, pp. 92, 93.

[10] Greenwood, D. T., *Principle of Dynamics*, 2nd ed., Prentice-Hall, Englewood Cliffs, NJ, 1988, pp. 362–363.

[11] Anon., *Handbook of Fiberglass and Advanced Plastic Composites*, edited by G. Luben, R. E. Krieger Publishing Co., Huntington, NY, 1969, pp. 303–305.

[12] Miller, I., and Freund, J. E., *Probability and Statistics for Engineers*, 3rd ed., Prentice-Hall, Englewood Cliffs, NJ, 1985, pp. 306–312.

[13] Hallquist, J. O., and Stillman, D. W., *LS-INGRID User's Manual*, Livermore Software Technology Corp., Waverly, CA, June 1991.

[14] Hallquist, J. O., *LS-Taurus Command Documentation Manual*, Livermore Software Technology Corp., Waverly, CA, April 1990.

[15] Hallquist, J. O., *LS-DYNA3D Theoretical Manual*, Livermore Software Technology Corp., Waverly, CA, June, 1991.

Earl A. Thornton
Associate Editor